

Preparation and characterization of indium oxide (In_2O_3) films by activated reactive evaporation

M D BENOY and B PRADEEP*

Department of Physics, Cochin University of Science and Technology, Kochi 682 022, India

MS received 7 February 1997; revised 11 August 1997

Abstract. The electrical and optical properties of In_2O_3 films prepared at room temperature by activated reactive evaporation have been studied. Hall effect measurements at room temperature show that the films have a relatively high mobility $15 \text{ cm}^2 \text{ v}^{-1} \text{ s}^{-1}$, high carrier concentration $2.97 \times 10^{20} / \text{cm}^3$, with a low resistivity $\rho = 1.35 \times 10^{-3} \text{ ohm cm}$. As-prepared film is polycrystalline. It shows both direct and indirect allowed transitions with band gaps of 3.52 eV and 2.94 eV respectively.

Keywords. Thin films; semiconductors; oxides; evaporation method.

1. Introduction

The simultaneous occurrence of high optical transparency and electrical conductivity is a rare phenomenon. The only way to obtain good transparent conductors is to create electron degeneracy in a wide band gap ($> 3 \text{ eV}$) oxide by introducing non-stoichiometry or appropriate dopants. Technological interest in transparent conductors has tremendously increased, since the first report of a transparent conducting cadmium oxide films by the thermal oxidation of sputtered cadmium by Badeker (1907).

Transparent conductors have found a variety of applications in electronic, optoelectronic and industrial devices such as solar energy conversion devices (Check *et al* 1978), gas sensors (Windischmann and Mark 1979), heat mirrors (Lampert 1981), laser damage resistant coatings in high power laser technology (Powlewicz *et al* 1979) etc. Oxides of In, Sn, Cd, Zn and their combinations are used as transparent conductors. Most of the research work has been concentrated on the oxides of In, Sn and their combinations because of the low cost and the high performance of these oxides. Different techniques have been used for the preparation of these oxide films. Commonly used preparation techniques are sputtering, electron beam evaporation, reactive evaporation and chemical spray method (Chopra *et al* 1983; Dawar and Joshi 1984). In most cases poly-crystalline films are obtained for a substrate temperature, ranging from 250°C – 400°C . Here we report the electrical and optical properties of polycrystalline indium oxide films prepared at room temperature by activated reactive evaporation.

2. Experimental

Indium oxide films were prepared by activated reactive evaporation using a resistively heated molybdenum boat in a conventional vacuum system. The evaporation is carried

* Author for correspondence

out in the presence of an oxygen plasma. The oxygen plasma was created inside the chamber, pumped with diffusion pump and rotary combination. The system was first evacuated to $\approx 10^{-5}$ Torr. Then industrial grade oxygen was admitted into the vacuum chamber through the needle valve, to a pressure $\approx 3 \times 10^{-4}$ Torr. Then the anode supply was turned on initiating the discharge. A bluish glow filled the whole chamber, and a steady discharge current was maintained. 5N purity indium was then evaporated to the oxygen plasma. A slight adjustment of the needle valve was necessary to maintain the oxygen pressure at $\approx 3 \times 10^{-4}$ Torr. The detailed experimental techniques have been reported elsewhere (George *et al* 1986).

Optically flat glass slides were used as substrates. Substrates were cleaned with an industrial detergent, followed by running water and 10 min ultrasonic agitation in distilled water. The substrates were dried with hot air and loaded into the chamber.

The rate at which the metal atom arrives at the unit area of a substrate can be expressed in terms of the deposition rate as observed from the same source at the same temperature and distance, but in the absence of oxygen flux (Glang 1970).

$$\frac{dN_m}{A_r dt} = \frac{N_a \rho_m d'}{M_m} \text{ atoms cm}^{-2} \text{ S}^{-1},$$

where N_a is the Avagadro number, ρ_m the density of the metal film in g cm^{-3} , M_m the molar mass of the metal in g mol^{-1} , A_r the reactive surface area in cm^2 and d' the deposition rate in cm/sec . The impingement rate of oxygen molecules is given by

$$\frac{dN_{O_2}}{A_r dt} = 3.513 \times 10^{22} (M_{O_2} T)^{-1/2} P_{O_2} \text{ cm}^{-2} \text{ S}^{-1},$$

where M_{O_2} is the molar mass of oxygen, T the vapour temperature (≈ 300 K) and P_{O_2} the oxygen partial pressure in Torr.

It has been found that the following deposition parameters give good quality films. Indium impingement rate $\approx 2.765 \times 10^{15}$ – 2.975×10^{15} $\text{atoms cm}^{-2} \text{ S}^{-1}$, oxygen impingement rate $\approx 1.0899 \times 10^{17}$ $\text{mol cm}^{-2} \text{ S}^{-1}$, substrate temperature = 300 ± 10 K and deposition rate ≈ 400 – 500 $\text{\AA}/\text{min}$.

Reproducible films were obtained under these conditions and were used for the optical and electrical studies. The films were identified using X-ray diffraction. The film thickness was measured by Tolansky's multiple beam interferometric method (Tolansky 1948). Films having thickness of the order of 3500 \AA were used for the electrical and optical studies. Conductivity and Hall effect measurements were carried out using conventional four-probe method. The electrical contacts were made using evaporated indium. The transmission spectra was recorded from 2600 nm to cut off using a Hitachi U-3410 UV-Vis-NIR spectrophotometer. The refractive index (n) and the absorption coefficient (α), of the films were calculated by the method developed by Swanepoel (1983).

3. Results and discussion

Figure 1 shows the X-ray diffraction pattern of indium oxide films prepared at room temperature. The d values and relative intensities for indium oxide given in the JCPDS card No. 6-416 along with our results are given in table 1. The peak corresponding to $d = 3.246$ \AA is an unidentified one.

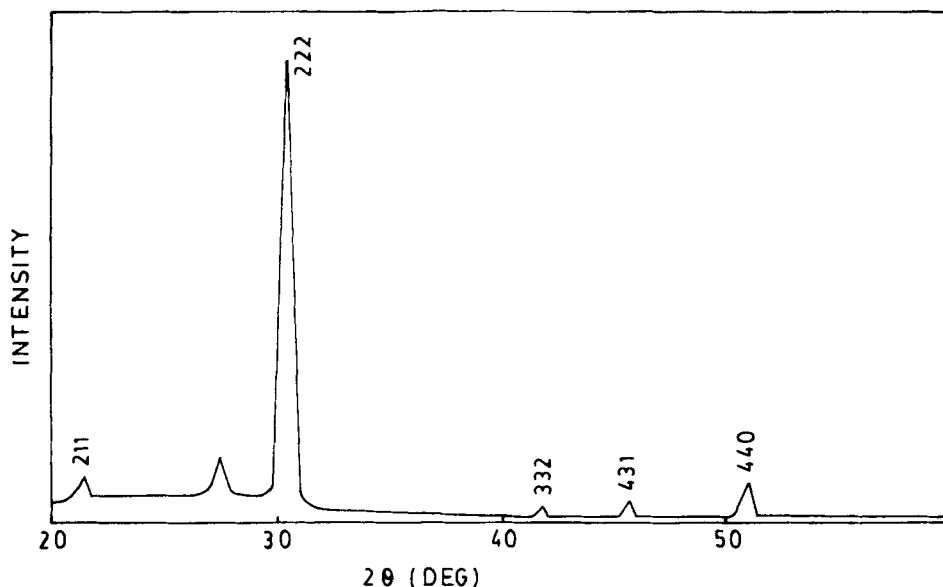


Figure 1. X-ray diffraction pattern of In_2O_3 thin film prepared at room temperature.

Table 1. X-ray diffraction data for the In_2O_3 thin film prepared at room temperature.

(hkl)	Standard pattern		Prepared film	
	$d, \text{A.u}$	I/I_0	$d, \text{A.u}$	I/I_0
211	4.130	14	4.148	9.8
...	3.246	14.0
222	2.920	100	2.919	100
332	2.157	6	2.159	3.16
431	1.984	10	1.983	3.9
440	1.788	35	1.789	9.1

3.1 Electrical properties

The conductivity and Hall effect measurements were carried out as a function of temperature ranging from room temperature to 353 K. It is observed that the films exhibit a metallic conduction. We obtained for instance an In_2O_3 film with resistivity $\rho = 1.35 \times 10^{-3} \Omega \cdot \text{cm}$, the mobility $\mu = 15 \text{ cm}^2 \text{ v}^{-1} \text{ s}^{-1}$ and carrier concentration $N = 2.97 \times 10^{20} / \text{cm}^3$ at room temperature.

Figure 2 shows the variation of conductivity (σ) with temperature (T). It is found that the conductivity decreases with increase in temperature. The $\ln \sigma$ vs $1/T$ relationship is linear and it consists of two linear portions. Thermal activation energy can be calculated using Arrhenius relation

$$\sigma = \sigma_0 \exp(-Q/KT),$$

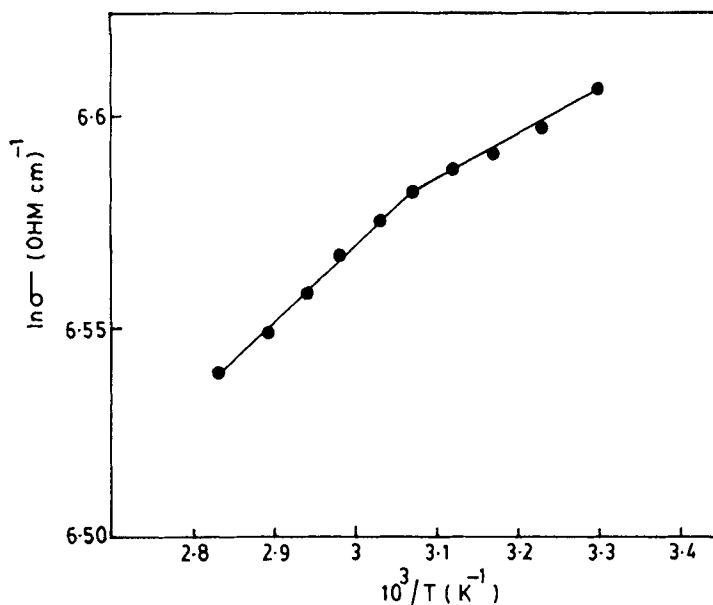


Figure 2. Variation of d.c. conductivity with temperature.

where Q is the activation energy, K the Boltzman's constant and T the absolute temperature. Here we get two activation energies, one corresponding to the low-temperature region and the other corresponding to the high-temperature region. At low-temperature region it is found to be 0.8×10^{-2} eV, which is sufficient to allow the hopping of ions into already existing vacancy sites. In the high-temperature region, the activation energy is found to be 1.5×10^{-2} eV. At high temperature additional vacancy sites are created, so the observed energy is the sum of the energy for vacancy creation and ion movement (Rolf 1985).

Figure 3 shows the variation of mobility with temperature. It is found that the mobility decreases with increase in temperature. The temperature dependence of mobility is related to the scattering mechanism of the free carriers. It is reported that the acoustical phonon scattering is a dominant mechanism in highly degenerate polycrystalline In_2O_3 films prepared by reactive sputtering (Fistul and Vainshtein 1967). Dependence of mobility on temperature also suggests another scattering mechanism viz. ionized impurity scattering due to the presence of oxygen vacancies and/or excess indium atoms, which results in a very high free carrier concentration of the order of 10^{20} cm^{-3} . Noguchi and Sakata (1980) reported that for In_2O_3 film, the mobility is independent of temperature in the range 77–300 K. We observed that the mobility decreases as the temperature increases in the range 300–353 K. It may be due to the lattice and/or ionized impurity scattering. Moreover the electrical properties of transparent conducting oxide films strongly depend on the method of preparation, oxygen partial pressure during the deposition etc.

Figure 4 shows the variation of Hall coefficient (R_H) with temperature (T). It is found that R_H is independent of temperature. This means that the film is degenerate (Hannay 1960). Further studies show that the film is n -type. The carrier concentration is found

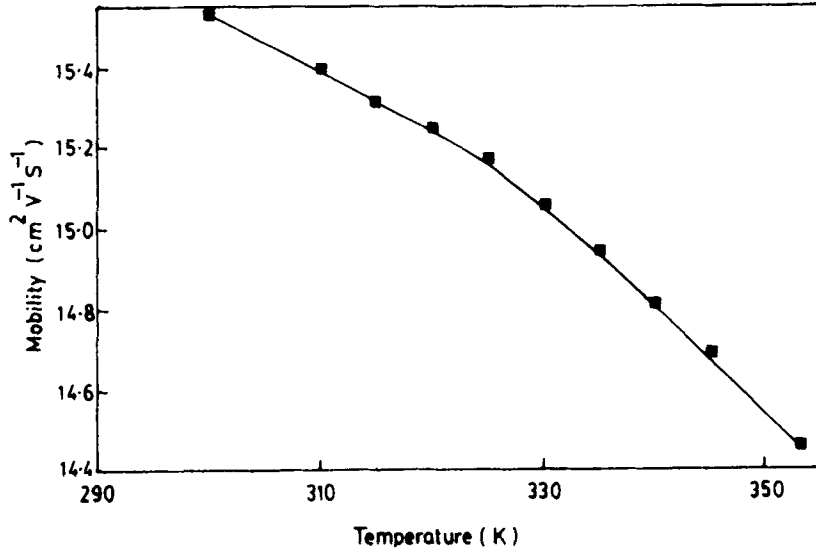


Figure 3. Variation of Hall mobility with temperature.

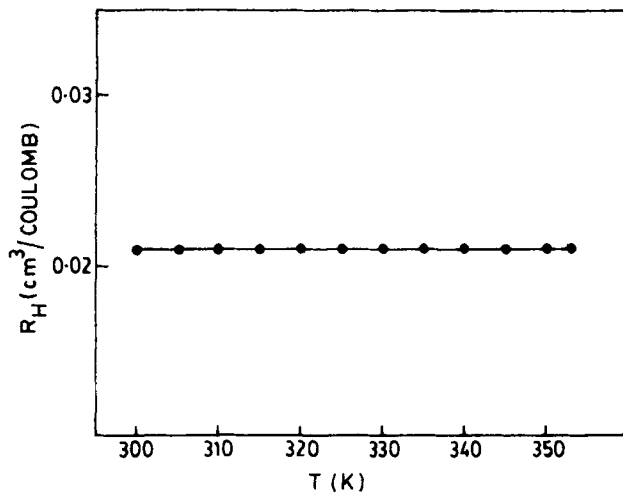


Figure 4. Variation of Hall coefficient with temperature.

to be $2.97 \times 10^{20} \text{ cm}^{-3}$ at room temperature. A completely oxidized In_2O_3 film has such a high value for the carrier concentration, which is excited thermally from the donor levels, originating from the defects near the bottom of the conduction band. The Fermi energy E_F can be evaluated using the formula

$$E_F = (\hbar^2/8m^*) (3N/\pi)^{2/3},$$

where m^* is the reduced effective mass and \hbar the planks constant. With $m^* = 0.3 m_0$ (Clanget 1973), we obtained $E_F = 0.54 \text{ eV}$. This is much greater than KT , 0.025 eV . This shows that the film is highly degenerate.

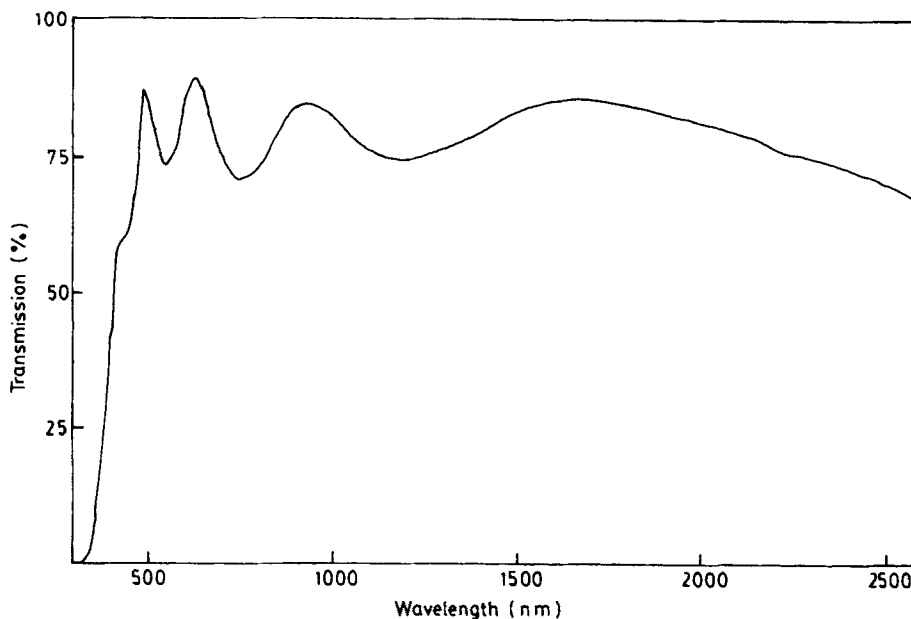


Figure 5. Transmission spectrum of a typical In_2O_3 thin film.

It is reported that the In_2O_3 film prepared at room temperature shows semiconducting behaviour (Nath *et al* 1980). But we observed that the In_2O_3 film shows a metallic behaviour. Here the decrease in conductivity is due to the fall in mobility, while the carrier concentration remains unchanged. Also, the lattice scattering can be predominant over ionized impurity scattering, because of the smaller grain size of the films prepared at room temperature (Chopra 1979).

3.2 Optical properties

The optical studies were done using films of thickness of the order of 3500 \AA , prepared on glass substrates. The refractive index (n) and absorption coefficient (α) of the films were calculated using the method of Swanepoel (1983).

Figure 5 shows the transmission spectrum of a typical In_2O_3 film prepared at room temperature. It shows an average transmittance of 80% over a wavelength range of 500–1680 nm. A sharp decrease in the transmittance at the lower wavelength region is due to the fundamental absorption and the decrease in transmittance at the higher wavelength region is due to the free carrier absorption (Mizuhashi 1980), a phenomenon that is common in all transparent conductors having high carrier concentration.

Figure 6 shows the variation of refractive index with the wavelength and it is found to be constant for wavelengths greater than 1000 nm.

Figure 7 shows the variation of absorption coefficient with the photon energy $h\nu$.

The absorption coefficient data was analysed by the theory of Bardeen *et al* (1956). Figure 8 shows the plot of $(\alpha h\nu)^2$ vs $h\nu$. This gives a band gap of 3.52 eV, leading to a direct allowed transition. This value is comparable with the band

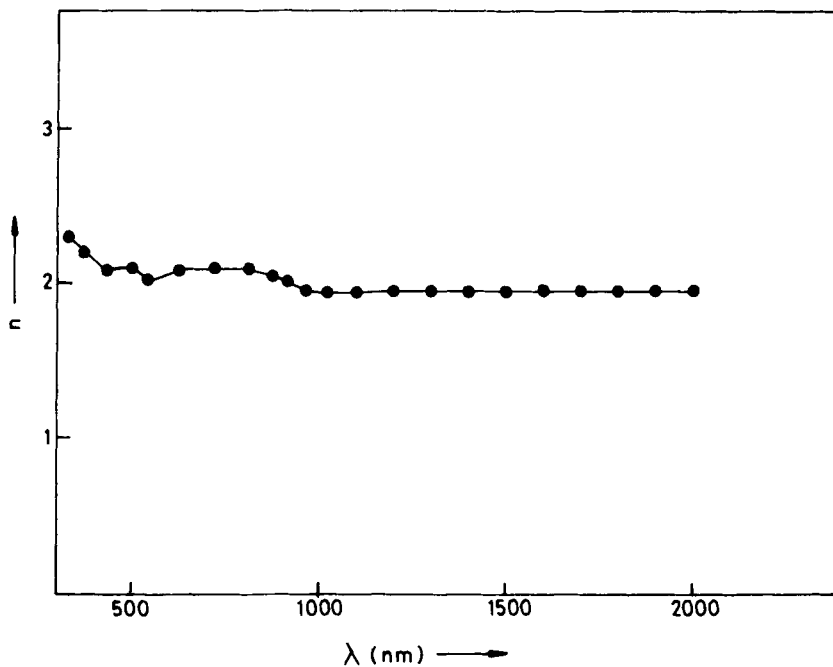


Figure 6. Variation of the refractive index (n) with the wavelength (λ).

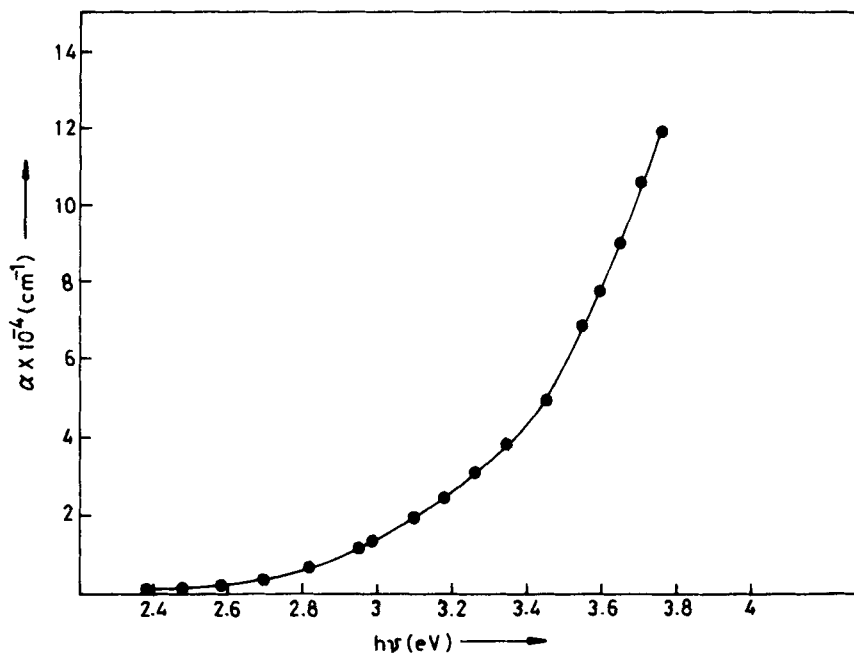


Figure 7. Variation of absorption coefficient (α) with the photon energy ($h\nu$).

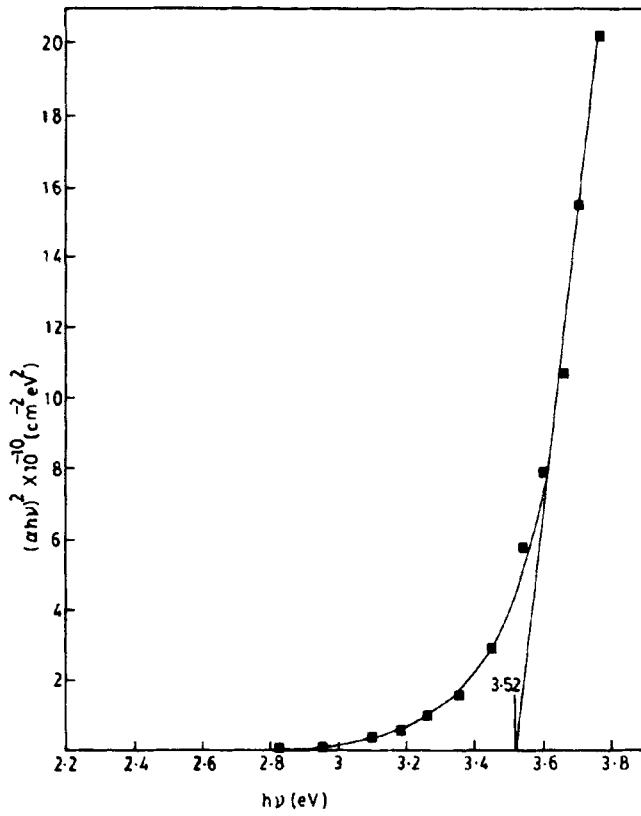


Figure 8. Variation of $(\alpha h\nu)^2$ against the photon energy ($h\nu$).

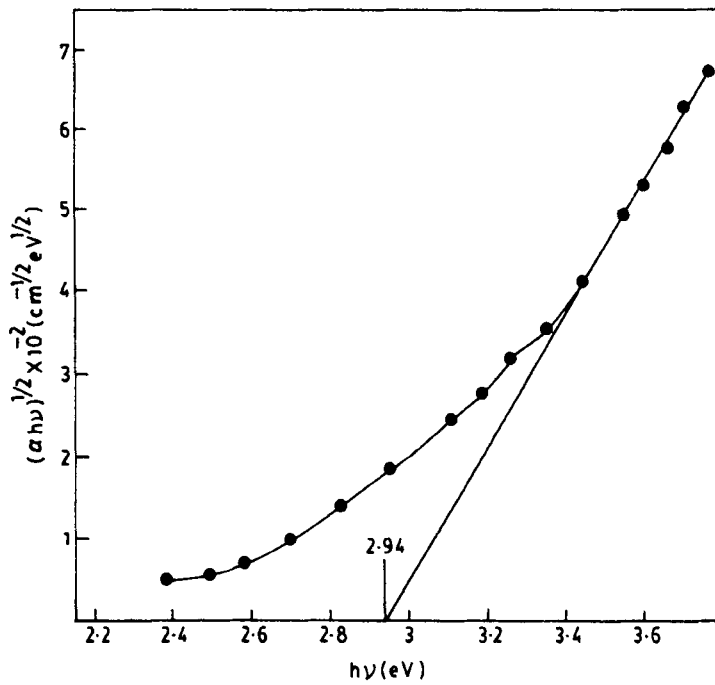


Figure 9. Variation of $(\alpha h\nu)^{1/2}$ against the photon energy ($h\nu$).

Table 2. Comparison of transparent conducting films prepared by different authors.

Material	Preparation technique	Sheet resistance (R_s) (ohms/ \square)	Mobility (μ) ($\text{cm}^2\text{v}^{-1}\text{s}^{-1}$)	Carrier concentration (N) (cm^{-3})	Transmittance ($T\%$)	Figure of merit (ϕ TC)	Reference
In_2O_3	Activated reactive evaporation (ARE)	38.6	15.5	2.97×10^{20}	80	2.78×10^{-3}	Present work
In_2O_3	Thermal evaporation	88	72	3×10^{20}	80	1.22×10^{-3}	Bardeen <i>et al</i> (1956)
$\text{In}_2\text{O}_3:\text{Sn}$	ARE	20	20-30	10^{21}	90	1.74×10^{-2}	Nath <i>et al</i> (1980)
$\text{In}_2\text{O}_3:\text{F}$	Ion plating	40	13	7×10^{20}	80	2.68×10^{-3}	Avaritiotis and Howson (1981)
$\text{In}_2\text{O}_3:\text{Sn}$	Spray	3.1	—	—	88	8.98×10^{-3}	Manificier <i>et al</i> (1979)

gap reported for bulk In_2O_3 (Jarzebski and Marlon 1976). Figure 9 shows the plot of $(\alpha hv)^{1/2}$ vs hv . This gives a band gap of 2.94 eV, corresponding to the indirect allowed transition, is also in agreement with the reported values (Weiher and Dick 1964).

4. Figure of merit

Usually the performance of transparent conductors are compared using the figure of merit (Hacke 1976) and is defined as

$$\phi_{\text{TC}} = \frac{T^{10}}{R_s},$$

where T is the transmittance and R_s the sheet resistance. A comparison of the performance of transparent conducting films prepared by various techniques is given in table 2.

5. Conclusion

Polycrystalline In_2O_3 films have been prepared at room temperature, by activated reactive evaporation. The film shows a low resistivity and high transmittance, which is comparable with that of the doped In_2O_3 films. It offers relatively high deposition rate, 450–500 Å/min and involves no post-deposition heat treatment, which makes this method attractive for the preparation of transparent conducting oxide films.

References

- Avaritsiotis J N and Howson R P 1981 *Thin Solid Films* **80** 63
 Badeker K 1907 *Ann. Phys. (Leipzig)* **22** 749
 Bardeen J, Blatt F J and Hall L H 1956 *Proceedings of photoconductivity conference, Atlantic city* (New York: Wiley)
 Check G, Inone N, Goodnick S, Genis A, Wilmsen C and Dubow J B 1978 *Appl. Phys. Lett.* **33** 643
 Chopra K L 1979 *Thin film phenomena* (New York: Robert E Krieger Publishing Company) p. 182
 Chopra K L, Major S and Pandya D K 1983 *Thin Solid Films* **102** 1
 Clanget R 1973 *Appl. Phys.* **2** 247
 Dawar A L and Joshi J C 1984 *J. Mater. Sci.* **19** 1
 Fistul V I and Vainshtein V M 1967 *Sov. Phys. Solid State* **8** 2769
 George J, Pradeep B and Joseph K S 1986 *Rev. Sci. Instrum.* **57** 9
 Glang R 1970 *Handbook of thin film technology* (eds L I Maissel and R Glang (New York: McGraw Hill Publishing Co) p. 1
 Hacke G 1976 *J. Appl. Phys.* **47** 4086
 Hannay N B 1960 *Semiconductors* (London: Chapman and Hall) p. 32
 Jarzebski J M and Marlon J P 1976 *J. Electrochem. Soc.* **123** 333 c
 Lampert C M 1981 *Sol. Energy Mater.* **6** 1
 Manificier J C, Szepessy L, Bresse J F, Perotin M and Stuck R 1979 *Mater. Res. Bull.* **14** 109
 Mizuhashi M 1980 *Thin Solid Films* **70** 91
 Nath P, Bunshah R F, Basol B M and Staffsud O M 1980 *Thin Solid Films* **72** 463
 Noguchi S and Sakata H 1980 *J. Phys.* **D13** 1129
 Powlewicz W T, Mann I B, Lowdermilk W H and Milam D 1979 *Appl. Phys. Lett.* **34** 196
 Rolf E H 1985 *Electronic properties of materials* (New York: Springer Verlag) p. 128
 Tolansky S 1948 *Multiple beam interferometry of surfaces and films* (London: Oxford University Press)
 Swanepoel R 1983 *J. Phys. E. Sci. Instrum.* **16** 1214
 Weiher R L and Dick B G 1964 *J. Appl. Phys.* **35** 3511
 Windischmann H and Mark P 1979 *J. Electrochem. Soc.* **126** 627